

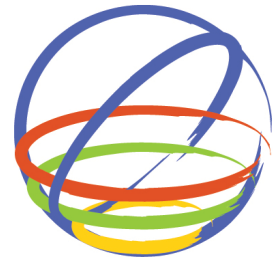
Formulation and validation of a macro-element for the equivalent frame modelling of internal walls in *Pombalino* buildings

H.A. Meireles, R. Bento

ICIST, Instituto Superior Técnico, Technical University of Lisbon, Portugal

S. Cattari, S. Lagomarsino

Department of Civil, Environmental and Architectural Engineering, University of Genoa, Italy



15 WCEE
LISBOA 2012

SUMMARY:

The heritage value of the mixed wood-masonry 18th century *Pombalino* buildings of downtown Lisbon is recognized both nationally and internationally. The present paper focuses on the formulation, implementation and validation of a macro-element for the internal walls (*frontal* walls) in *Pombalino* buildings in a structural software called Tremuri (originally developed at the University of Genoa from 2002). This program works according to the equivalent frame approach; it allows analysing complex 3D models by performing non-linear analyses with a reasonable computational effort. In particular, the macro-element developed is obtained based on the development of a hysteretic model based on phenomenological laws aimed at reproducing the behaviour of the walls under general monotonic, cyclic or earthquake loading. The model is based on a minimum number of path following rules and is constructed using exponential and linear functions. The model parameters are calibrated with experimental data. As an example a complete *Pombalino* building is modelled and analyzed by non linear static analyses. The structure is modelled using non-linear beams for the masonry panels and for the *frontal* walls. The results are compared in terms of pushover curves.

Keywords: *Pombalino* buildings, macro-element, frontal walls, equivalent frame model

1. INTRODUCTION

The heritage value of the mixed wood-masonry 18th century *Pombalino* buildings in downtown Lisbon is recognized both nationally and internationally. In 1755 a catastrophic earthquake followed by a major tsunami struck the capital of Portugal causing severe damage to the city. The event completely destroyed the heart of the city, which was set on a valley area close to the river Tagus and is composed of a shallow layer of alluvial material. The disaster required an urgent solution. The Prime Minister at the time, Marquis of *Pombal*, was set in charge of rebuilding the city and restoring it back to normality as fast as possible. He delegated to a group of engineers the development of a structural solution that would guarantee the required seismic resistance of the buildings. Based on the know-how of that time and on the empirical knowledge gathered from the buildings that survived the earthquake a new type of construction was created, which is now generally referred to as *Pombalino* construction. An example of the construction elements that compose a *Pombalino* building can be seen in Fig. 1.1.

Based on Mascarenhas (2005), the following can be said. The buildings were built in quarters comprising each quarter an average of 10 buildings. The foundation system was ingenious; it is based on a system of wooden piles over the alluvium layers. The piles are similar and repetitive, on average 15 cm in diameter and 1.5 m in length. These form two parallel rows in the direction of the main walls, which were linked at the top by horizontal wood cross-members attached by thick iron nails. The construction at ground floor consisted of solid walls and piers linked by a system of arches. In more elaborate cases, thick-groined vaults spanned between the arches, which protected the upper floors from the spread of any fire that might start at ground floor level. From the first floor up the basis of this building system is a three-dimensional timber structure called *gaiola* (cage), thought to be an improved system based on prior traditional wooden houses. The *gaiola* is composed of traditional timber floors and improved mixed timber-masonry shear walls (*frontal* walls) that would support not

only the vertical loads but also act as a restrain for the seismic horizontal loading. However, no analytical models with any structural software have proven that so far and we have to assume the current lack of knowledge in predicting the role of these *frontal* walls in the seismic resistance of the buildings. Nevertheless, these *frontal* walls are one of the main speciousness of these buildings. They consist of a wooden truss system filled with a weak mortar in the empty spaces (Fig. 1.2.). Finally, the buildings are encompassed by façade and gable walls made of stone and rubble masonry. These walls decrease thickness in height. The gable walls are shared between adjacent buildings.

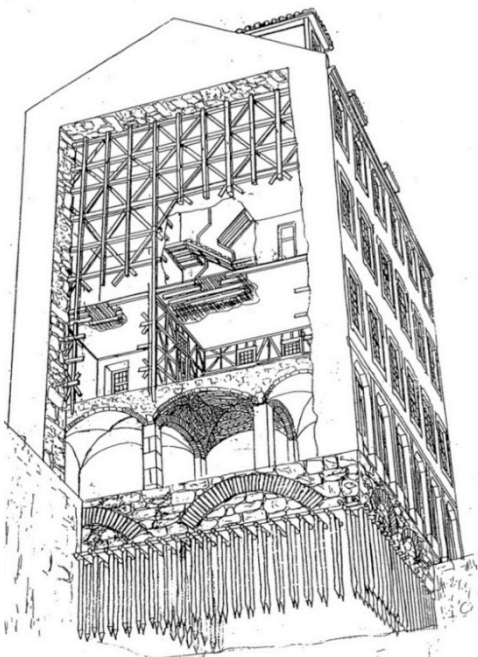


Figure 1.1. Example of a *Pombalino* building (Mascarenhas, 2005)

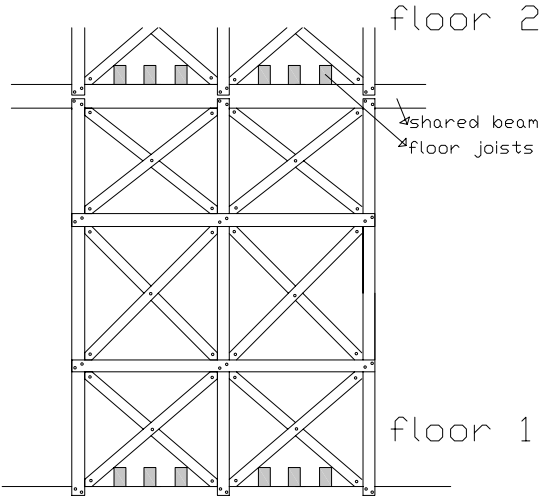


Figure 1.2. Drawing of a *frontal* wall and its connection to the above floors

The work of Meireles and Bento (2010) was the first to test the *frontal* walls under static cyclic shear testing with imposed displacements, where a specific loading protocol was used and vertical loading applied to the specimen by four hydraulic jacks and rods. The objective of the experimental work developed in the cited paper was, therefore, to obtain the hysteretic behaviour of these *frontal* walls, by means of static cyclic shear testing with imposed displacements. These properties shall be used in developing a specific hysteretic model for *frontal* walls, which is the scope of the present paper.

2. MACRO-ELEMENT

The element developed (see Meireles *et al.*, 2011) was a non linear beam with a hysteretic behaviour for the shear response on phenomenological basis. This hysteresis rule developed is defined by 9 independent physical or mathematical parameters and incorporates stiffness and strength degradations and pinching effect. The associated hysteresis rule is developed based on the experimental tests carried out (Meireles and Bento, 2010) and the parameters are calibrated by such results.

2.1. Hysteresis model

A hysteresis model was developed based on a minimum number of path-following rules that can reproduce the response of the wall tested under general monotonic, cyclic or earthquake loading. As referred, the model was calibrated according to the experimental results obtained. It was constructed using a series of exponential and linear functions. This model uses 9 parameters to capture the nonlinear hysteretic response of the wall: a first set of parameters aimed to define the envelope curve ($F_0, K_0, r_1, r_2, F_u, \delta_{ult}$); two parameters to define the unloading curve (α, λ_u); a last one to define the reloading curve (a). Fig. 2.1. shows the assumed hysteresis model of the wall.

The first step for obtaining a hysteresis model is to define the envelope curve. It is assumed that the envelope curve is independent of the loading history and coincides approximately with the load-deformation curve obtained under monotonic loading. Once the envelope is determined the loading and unloading paths must be described. Loading (or reloading) paths are identified as cases where the displacement, δ , and the gradient of the displacement, $\Delta\delta$, both have the same signs ($\delta*\Delta\delta>0$). In contrast, unloading paths correspond to cases where the displacement and the gradient of the displacement have opposite signs ($\delta*\Delta\delta<0$).

The path-following rules are such that the structure loaded in the first cycle will draw the envelope curve. The monotonic response of the wall (envelope curve) is modelled using one exponential and one linear function. The exponential function defines the ascending branch (*exponential envelope*) and the linear function the descending branch (*linear envelope*). The envelope curve is defined by 6 identifiable parameters that must be fitted to experimental data. It follows an unloading path at a certain point and the loading in the opposite direction. A linear loading branch is defined in the model so as to have a transition between the point Z (Fig. 2.1.) and the envelope curve when the structure is loaded in the opposite direction for the first time. Afterwards, when the structure is loaded again in the initial direction, it will reload with a linear reloading path, which is not the same as the envelope path. When the structure's reloading path reaches the envelope curve it means the structure is being loaded for the first time for those displacements; then, the envelope curve is followed again. Once more, unloading can happen at any point. To better match the experimental results and based on the observation of these, the unloading has an initial exponential branch until the zero force intercept followed by a linear unloading branch until the zero displacement intercept, point Z. Additionally, the experimental results reveal a degrading unloading stiffness if one considers this stiffness to be K_u . This degradation is related to the point of the start of the unloading δ_{ou} ; the unloading stiffness is decreasing with increasing values of δ_{ou} . An exponential function that is capable of capturing this fact has been defined.

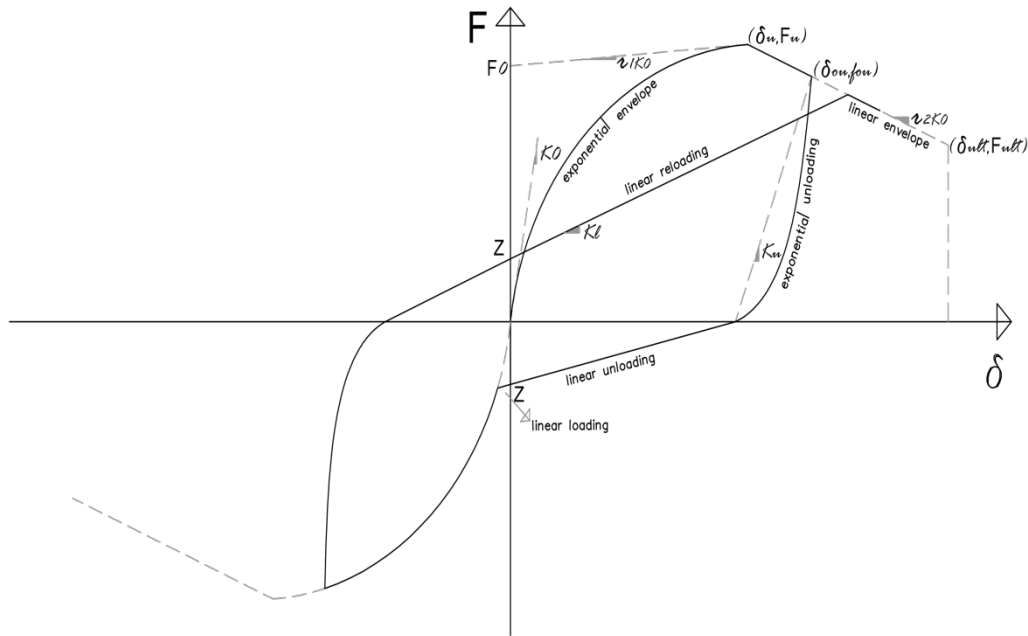


Figure 2.1. Hysteresis model

One important characteristic that could be observed in the response of these walls is the degradation of the restoring force, commonly known as strength degradation. In this situation, it is observed that the reloading curve does not reach the point of maximum displacement at the envelope curve but instead points to a point that is lower by a certain amount of force (for instance a). As a consequence, the stiffness also decreases by a certain amount, or it degrades (stiffness degradation). The strength degradation in the model was estimated by calculating the force reduction parameter a for each level of damage. The damage is assumed to be related to the maximum displacement (or the maximum drift) attained so far and is a variable that is calculated at each loop based on the whole history of the force-displacement response. In this way, a linear reloading curve is drawn from the point Z to the damaged point. At the beginning of a reloading path the initial point at y-intercept, Z , is known. The force reduction parameter a is calibrated based on the experimental results and is not a fixed parameter since it varies according to the damage built up in the structure. Strength degradation is thus estimated directly but stiffness degradation is accounted for indirectly in this modelling technique. In other models, however, strength degradation is accounted for indirectly.

The rules previously described define complete loops, which are loops that undergo complete unloading. In order to have a more general model, one that could be subjected to any type of loading, and not restricted to cyclic loading, one needs to account also for situations where reloading can happen at any place during the loading/unloading history. This leads to small cycle or incomplete cycle hysteresis. In the proposed model herein defined, because of the lack of any other information or data, it was simply assumed that the structure would reload with a linear branch until it would reach the previously defined linear reloading branch. This would happen both if the reloading would take place at the exponential unloading branch or at the linear unloading branch. The new linear branch defined has the derivative K_0 , equal to the initial stiffness.

3. EXPERIMENTAL VERSUS ANALYTICAL HYSTERESIS

A plot has been drawn for comparison of the hysteresis curves obtained experimentally and the hysteresis curve developed analytically. A good matching is obtained as can be seen in Fig. 3.1. The legend "Exp SC2" and "Exp SC3" are the experimental results obtained while the legend "Numerical" is the hysteresis curve developed analytically.

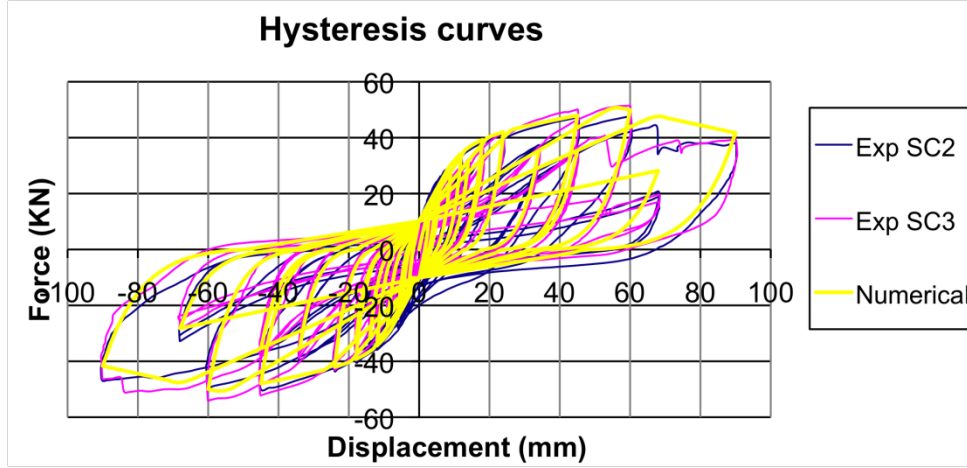


Figure 3.1. Experimental versus analytical hysteresis

The accuracy of the model response is determined using one error indicator, which is the cumulative energy error (CEE). The CEE is defined as in Eqn. 3.1.

$$CEE = \frac{|CE_{test} - CE_{anal}|}{|CE_{test}|} \quad (3.1.)$$

Where CE_{test} and CE_{anal} are the cumulative energy dissipation of the hysteresis of the experimental testing and of the analytical model, respectively. The cumulative energy dissipated by the wall, CE , is calculated as in Eqn. 3.2.

$$CE = \sum_i \int_{\delta_{i-1}}^{\delta_i} F(\delta) d\delta \approx \sum_i \frac{F_i + F_{i-1}}{2} (\delta_i - \delta_{i-1}) \quad (3.2.)$$

Where the subscript i is the i^{th} force-displacement (F - δ) data point. The total percent error in cumulative energy dissipated between the fitted model and the actual cyclic test data is 9% for the test SC2 and 14% for the test SC3, indicating a good match between the analytical model and the experimental results.

4. CASE-STUDY

The current section focuses on the modelling and on the seismic assessment of a typical Pombalino building with a structural software able to perform nonlinear static and dynamic analyses where the previously described element has been incorporated. The program used is Tremuri which has been originally developed at the University of Genoa, starting from 2002 (Galasco *et al.* 2009), and subsequently implemented in the software package 3Muri (release 4.0.5, which has been used to generate the 3D model). In particular, it works according to the equivalent frame approach. Thus, each wall is discretized by a set of masonry panels (*piers* and *spandrels*), in which the non-linear response is concentrated, connected by a rigid area (*nodes*), whereas floors are modelled as orthotropic membrane finite elements. Model focuses only to the global building response (which is assumed to be governed only by the in-plane behaviour of walls), the local flexural behaviour of floors and the out-of-plane walls' response are not explicitly computed. For further details see also Galasco *et al.* (2004) and Lagomarsino and Cattari (2009). The structure is modelled by using non-linear beams for both the ordinary masonry panels and the *frontal* walls (according to the hysteretic behaviour formulation described in paragraph 3). By using Tremuri, non linear static analyses were performed and the capacity curves in both directions evaluated.

4.1. Typical *Pombalino* building

The building that was chosen to be analysed in this study tries to replicate a typical *Pombalino* building. On the other hand, it was searched also a building in Lisbon downtown that had been the subject of previous analysis and evaluation so that information would be available with respect to the plan architecture of the building. In this way, it was found a building that had been the subject of research in the study of Cardoso (2003). This existing building is located in the numbers 210 to 220 of Rua da Prata and the historical background and architectural drawings are also present in the book *Baixa Pombalina: Passado e Futuro* (Pombaline downtown: Past and Future) (Santos, 2000). This building is recognized by the existence of a pharmacy in the ground floor, which is covered by a well-decorated panel of blue tiles, dating from 1860. Nevertheless, as is usual in the *Pombalino* buildings of downtown, this building has been subject of some alterations with respect to the original layout. In this particular case one floor has been added to the original layout of 4 floors plus roof, making a total number of 5 floors plus attic. In the present study, given that it is intended to study a typical *Pombalino* building, only 4 floors plus roof was considered in the layout, being the last floor below the roof eliminated in the drawings and modelling.

The building has six entries on the main façade and a height of approximately 15 m until the last floor (without the height of the roof). The openings have a width of 1.66 m, the door at the ground floor a height of 3.5 m, the balcony at the first floor a height of 3 m and the windows at the second and third floors a height of 2 m. At the back the openings are smaller and have a width of 1 m. At ground floor the height of the door is 3 m and at first, second, and third floors there are windows of 1.5 m high. There are only 5 entries. The plan drawings of the building are shown in Fig. 4.1. and Fig. 4.2. for the ground floor and upper floors, respectively.

The plan of the building has dimensions 18x11 m² referred to the façade and gable walls, respectively. The ground floor has 5 internal piers of dimensions 0.7x0.7 m². There are stairs in the middle of the building facing towards the back façade. These have brick masonry staircases only at ground floor (at the upper floors the staircases are *frontal* walls) of thickness 0.24 m. On the ground floor, the staircase brick masonry walls go further until the front of the building with a small misalignment towards the right. On the ground floor, the front and back façade piers as well as the internal piers are made of stone masonry. The gable walls as well as the front and back façades of the upper floors are constituted of rubble masonry.

On the upper floors (from the first until the third floor) one can find the *frontal* walls. There are two alignments of *frontal* walls parallel to the façades and five alignments (including the staircase) of *frontal* walls parallel to the gable walls. Connecting the *frontal* walls there are openings (doors) of 0.8 m. The actions considered on the structure are the self-weight loads given by the weights of the roof, the floors, the ceilings, the partition walls and the *frontal* walls themselves combined with the live loads respectively given by the Eurocode 1 (CEN, 2002). Table 4.1. summarizes the geometrical data and masonry types assigned to structural elements and actions considered in the model. From this table, the external walls (façade and backwards) are reducing their thickness towards height, being of 0.90 m on the ground floor and 0.75 m on the third floor.

The building has been modelled in the Tremuri software. The mechanical characteristics of the masonry types used are presented in Table 4.2. These values were obtained from the Italian Code for Structural Design (2008) and its Instruction Document (Circolare 2 febbraio, 2009, n. 617, table C8A.2.1) where for various types of masonry a range for the mechanical characteristics is proposed. It was decided, after selecting the masonry types to be adopted, to use the mean value of each class. Herein for stone masonry and brick masonry types, it has been assumed mechanical properties representative of a cracked condition (by assuming a 50% reduction factor for the Young Modulus E and the Shear modulus G). For the case of the rubble masonry this does not happen since it was also consulted another source of information for the obtainment of the Young Modulus (E). This has been some experimental testing carried out on one gable wall at ground floor on a buildings at downtown

that was being demolished (Pompeu Santos, 1997). The value obtained herein for E was about 1000 MPa being in accordance with the value of the chosen class of masonry - rubble masonry - with uncracked stiffness as can be seen in Table 4.2., second row.

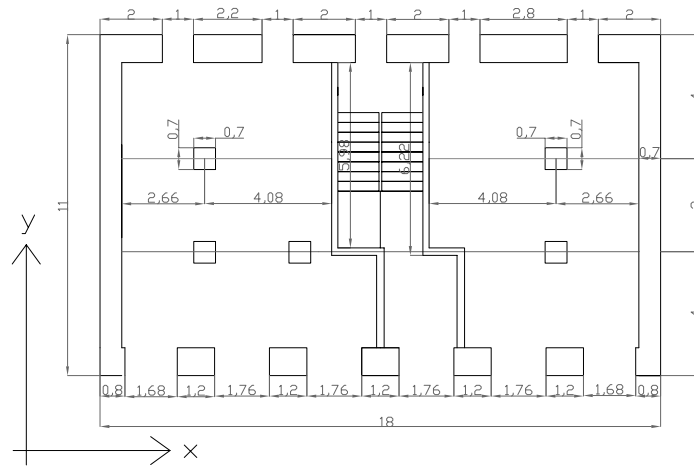


Figure 4.1. Sketch of the plan view of building: ground floor – units in metres

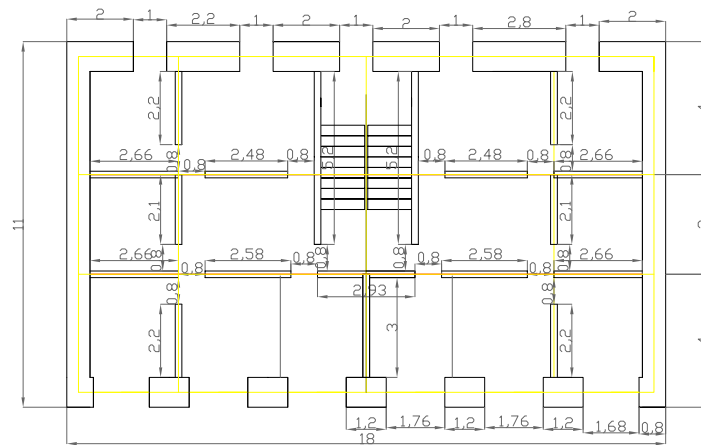


Figure 4.2. Sketch of the plan view of building: upper floors – units in metres

Table 4.1. Thickness and material of building components and actions considered

Geometrical data and masonry types			Actions considered		
Element	Material*	Thickness	Element	Location	Value**
Piers (ground floor)	SM	0.7x0.7 m ²	-	Floors	2 kN/m ² (<i>ll</i>)
External walls (façade and backwards):			-	Stair floor	4 kN/m ² (<i>ll</i>)
Ground floor	SM	0.90 m	Stairs	Stair floor	0.7 kN/m ² (<i>dl</i>)
1° floor	RM	0.85 m	Compartment walls	Floors	0.1 kN/m ² (<i>dl</i>)
2° floor	RM	0.80 m	Wooden floors	Floors	0.7 kN/m ² (<i>dl</i>)
3° floor	RM	0.75 m	Ceilings	Floors	0.6 kN/m ² (<i>dl</i>)
Spandrels	RM	0.20 m	“Frontal” wall	“frontal” walls	3.0 kN/m (<i>dl</i>)
Gable walls	RM	0.70 m	Vaults	Masonry walls ground floor	3.5 kN/m (<i>dl</i>)
Staircase (ground floor)	BM	0.24 m	Gable walls roof	Masonry walls 4th floor	17.3 kN/m (<i>dl</i>)
Internal walls (ground floor)	BM	0.24 m	Roof	Masonry walls 4th floor	4.4 kN/m (<i>dl</i>)

*SM, RM and BM mean stone masonry, rubble masonry and brick masonry, respectively
 **the load type is summarized in brackets: if live load (*ll*) or dead load (*dl*), respectively

Table 4.2. Mechanical characteristics of masonry types

Masonry type	Average Young Modulus E [GPa]	Average Shear Modulus G [GPa]	Weight W [KN/m ³]	Average Compressive Strength f_m [MPa]	Average Shear Strength τ_0 [MPa]
Stone Masonry	2.8*	0.86*	22	7	0.105
Rubble Masonry	1.23	0.41	20	2.5	0.043
Brick Masonry	1.5*	0.5*	18	3.2	0.076

* cracked stiffness assumed, 50% of the value used

The mechanical characteristics of the wood considered in this work are presented in Table 4.3. The joists of the floors have a section of 10x20 cm² and the wood pavement a thickness of 2 cm. In this basic configuration, the stiffness contribution of floor is mainly related to the pavement contribution: thus, they result as quite flexible orthotropic membrane finite elements. The stairs have been modelled as floors having the following cross sections: 10x10 cm² for the joists and 2 cm for the pavement. The joists run every 30 cm for both stairs and floors. In order to model the connections between *frontal* walls (referring to the top of the internal doors), in every floor, a timber beam has been included with section 10x10 cm². In reality, and depending on the quality of the construction, on the ground floor level there may exist quadripartite vaults, normal vaults or no vaults at all or only timber beams making the ground floor structure. The chosen modelling approach has been to model only timber beams on the ground floor. However, the weights of the vaults have been considered in the analysis as presented in Table 4.1. The cross section of the timber beams considered has a width of 20 cm and a height of 30 cm.

Table 4.3. Parameters adopted for the wood in *frontal* walls and floors

E_{wood} (MPa)	12000
ρ_{wood} (kg/m ³)	580
ν	0.2

Figure 4.3. shows a view of the 3D model and the equivalent frame idealisation in case of the front façade (where piers, spandrels and rigid nodes are marked in red, green and blue ciano, respectively). Herein, it is represented in grey the parts of the structure that are composed of rubble masonry; in purple the parts of the structure that are composed of stone masonry; in green (dark and light depending on the size) are the *frontal* walls and in light brown are the timber beams connecting the *frontal* walls.

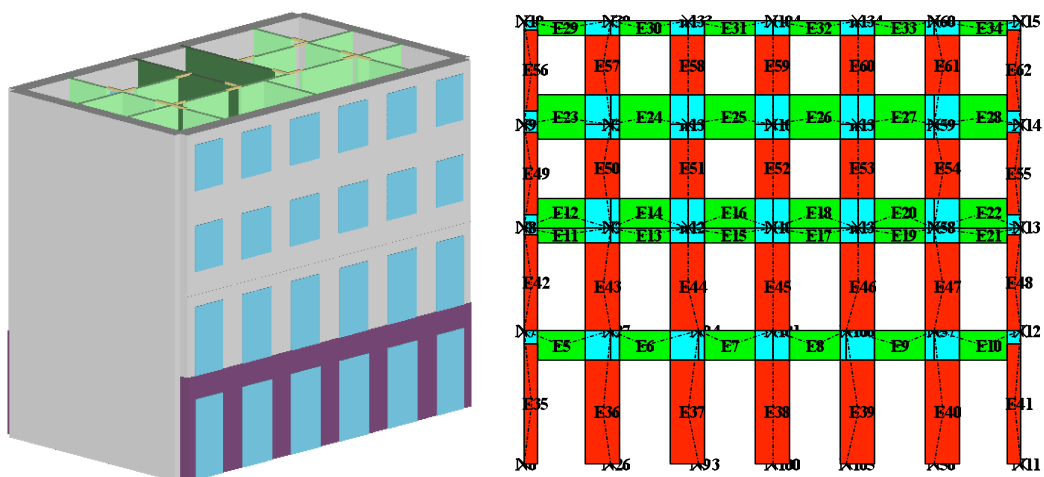


Figure 4.3. View of 3D model (left) and equivalent frame idealisation of front facade (right)

5. CAPACITY CURVES

Pushover analyses were carried out for both xx and yy directions and for two lateral load patterns: proportional to the mass (uniform); proportional to the mass and height (triangular). The pushover curves obtained are presented in Fig. 5.1.

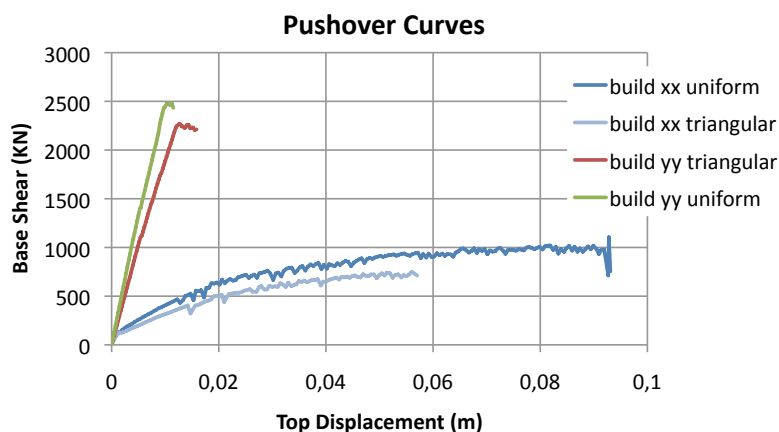


Figure 5.1. Pushover curves in the two directions for both uniform and triangular load patterns

Based on the results obtained it is evident that the stiffness and strength is much higher in the yy direction than in the xx direction: actually, no opening is present in two perimeter walls of the yy direction. On the other hand, the ductility of the system is much higher on the xx direction and is practically non-existing in the yy direction. Actually, in xx direction piers are very slender (due to the opening's configuration) and with a very moderate coupling provided by spandrels (which show a "weak" behaviour due to the lack of other tensile resistant element coupled to them): thus, a prevailing flexural response occurs associated to higher drift than in case of the shear failure. In general the structure exhibits a soft storey failure mode; moreover, since floors are quite flexible, a very moderate redistribution of seismic loads may occur among masonry walls. Comparing the results obtained with the two lateral load patterns, it can be seen how the mass x height load pattern (triangular) is more demanding than the load pattern proportional to the mass only (uniform load pattern), since the curves run below the later ones. Nevertheless, the difference between these two load patterns is not so substantial. Further issues focused on the repercussions on the seismic assessment are discussed in a companion paper of this conference (Meireles *et al.* 2012).

6. CONCLUSIONS

A new hysteretic model for wood *frontal* walls has been developed. This is the first hysteretic model developed in the literature for such walls. The hysteretic model is governed by path-following rules and is composed of linear and exponential functions. It is governed by 9 identifiable parameters. These parameters have been calibrated with experimental test results. The total percent error in cumulative energy dissipated between the fitted model and the actual cyclic test data is 9% for the test SC2 and 14% for the test SC3, accounting the good performance of the model. The model developed also accounts for characteristics such as pinching effect, strength and stiffness degradation that have been observed in the experimental data. The results obtained herein are essential for further work in modelling the behaviour of such walls under monotonic, cyclic or earthquake loading.

In the present paper a *Pombalino* building was modelled with both external masonry walls and internal *frontal* walls in the same structural model. This is original research and an accomplishment of the present work. The element formulated for *frontal* walls has been implemented in the Tremuri software which enables the nonlinear modelling of the masonry buildings. Thus nonlinear static analyses were carried out in the *Pombalino* buildings.

The *frontal* walls may play the role of preventing the out-of-plane failure of the masonry façades if they are properly attached to these walls. It has been assumed in the modelling that this is the case and that the out-of-plane failure is prevented both by the proper connections of the *frontal* walls to the masonry façades. The out-of-plane failure mode is thus not evaluated in this study but is instead assumed to be prevented by the proper connection between structural elements. Furthermore, the local out-of-plane mechanisms may be verified apart through suitable existing methods (see Magenes, 2006). In this way, it has been assumed that the building in its original state has good connections between structural elements (*frontal* walls, floors and masonry walls). However, in reality this may not be the case. It is important then to improve these connections in any intervention that would be performed on these buildings. It should be noticed also that, as a consequence, the buildings in reality might be even more vulnerable to seismic actions than the considered original building in this study. On the other hand, in the existing building stock in Lisbon downtown, there are many buildings which have been subjected to structural changes. These changes are, for example, removing ground floor masonry walls to have open spaces, removing façade pillars to have a larger entrance or removing *frontal* walls in the above floors. In this way, it is possible to understand that these altered buildings are even more vulnerable than the building evaluated in this study.

ACKNOWLEDGEMENT

The authors would like to acknowledge the financial support of the Portuguese Foundation for Science and Technology (Ministry of Science and Technology of Portugal) through the research project PTDC/ECM/100872/2008 and through the PhD scholarship SFRH/BD/41710/2007.

REFERENCES

- Eurocode 1: Actions on structures - Part 1-1: General actions -Densities, self-weight, imposed loads for buildings, EN 1991-1-1, (2002), Commission of the European Communities (CEN), Brussels.
- Circolare 2 febbraio, (2009), n. 617, Ministero delle Infrastrutture e dei Trasporti. /Istruzioni/ /per l'applicazione delle "Norme Tecniche per le Costruzioni" di cui al D.M. 14/01/2008/. G.U. n. 47 del 26/2/09 suppl. ord. n. 27 (In Italian). Cardoso M. R. P., (2003), Vulnerabilidade Sísmica de um Edifício Pombalino, Master Thesis, (IST), The Technical University of Lisbon. (in Portuguese).
- Galasco A., Lagomarsino S., Penna A. and Resemini S. (2004), Non-linear Seismic Analysis of Masonry Structures, *Proc. of 13th World Conference on Earthquake Engineering*, Vancouver 1-6 August, paper n. 843.
- Galasco A., Lagomarsino S., Penna A. and Cattari S. (2009), TREMURI program: Seismic Analyses of 3D Masonry Buildings, University of Genoa (mailto:tremuri@gmail.com).
- Italian Code for Structural Design (2008), D.M. 14/1/2008, Official Bulletin no. 29 of 4/02/2008 (In Italian).
- Lagomarsino S. and Cattari S. (2009), Non linear seismic analysis of masonry buildings by the equivalent frame model", *Proc. of 11th D-A-CH Conference*, 10-11 September 2009, Zurich, (invited paper), Documentation SIA D 0231, ISBN 978-3-03732-021-1.
- Magenes G, (2006), Masonry building design in seismic areas: recent experiences and prospects from a European standpoint, *First European Conference on Earthquake Engineering and Seismology*, Geneva Switzerland.
- Mascarenhas J., (2005), Sistemas de Construção V-O Edifício de rendimento da Baixa Pombalina de Lisboa, *Materiais Básicos 3º Parte: O Vidro*. Livros Horizonte (in Portuguese).
- Meireles H., Bento R., (2010), Cyclic behaviour of Pombalino "frontal" walls, *Proc. 14th European Conference on Earthquake Engineering*, pp.325, Ohrid, Macedonia.
- Meireles H, Bento R, Cattari S, Lagomarsino S, (2011), The proposal of a hysteretic model for internal wooden walls in Pombalino buildings, *Proc. of the 2011 World Congress on Advances in Structural Engineering and Mechanics (ASEM11plus)*, Seoul, South Korea.
- Meireles H, Bento R, Cattari S, Lagomarsino S, (2012), Seismic assessment and retrofitting of *Pombalino* buildings by fragility curves, *Proc. of the 15th World Conference on Earthquake Engineering*, Lisbon, Portugal.
- Pompeu Santos, (1997), Ensaios de Paredes Pombalinas. Nota Técnica N°15/97, NCE/DE, LNEC Lisboa (in Portuguese).
- Santos M. H. R., (2000), A Baixa Pombalina: Passado e Futuro, Livros Horizonte, Lisboa. (in Portuguese)
- 3Muri Program, release 4.0.5, <http://www.stadata.com>.